Thermoplastic polyurethanes with polycarbonate soft phase: Effect of thermal treatment on phase morphology

Thermoplastic polyurethanes with polycarbonate soft phase: effect of thermal treatment on phase morphology.

Elisa Cipriani, Marco Zanetti, Valentina Brunella, Luigi Costa, Pierangiola Bracco.

Dipartimento di Chimica and NIS Centre of Excellence, University of Torino, Italy

Corresponding author:

Marco Zanetti

marco.zanetti@unito.it

Via Pietro Giuria 7, 10125, Torino, Italy

Tel: +390116707547, Fax: +390116707855

Abstract

In this work the thermal sensitivity of thermoplastic polyurethanes with polycarbonate soft phase is considered (PCU). Thermal treatments were coupled with differential scanning calorimetry and infrared spectroscopy to investigate the effect of the temperature on the phase morphology. PCU is characterized by biphasic morphology: ordered hard polyurethane micro-domains are dispersed in a soft phase matrix, containing both hard and soft segments. The heating may completely destroy the short and long range order or simply change them. The infrared behaviour of the CO and NH stretching regions gives information on the organization of the segments. Thermal treatments over the processing temperature lead to an unstable monophasic morphology, that at ambient temperature is subjected to segregation process of the hard segments, in order to create again the biphasic morphology. Annealing treatments below the processing temperature cause reorganization in the hard micro-domains, inducing changes in their amount and dimensions. The result of the annealing depends on the temperature and on the exposition time. The thermal sensitivity regards also the chemical properties, given the thermal lability of the urethane bonds in the range of the processing temperature.

Keywords

Poly carbonate urethane, Processing, Morphology, DSC, FT-IR

1. Introduction

The interest in polyurethanes belongs from their heterogeneity in chemical and physical properties. Thanks to the opportunity to incorporate other functional groups in the polymer network, producing varied copolymers, polyurethanes properties may range from rigid hard thermosetting materials to softer elastomers. Thermoplastic polyurethanes (TPUs) combine the elastomeric behaviour with the possibility to be processed with conventional thermoplastic machinery. Thanks to the large range and exceptional mechanical properties, TPUs have many uses that cover medical technology, shoes manufacturing, car industry and many others [1].

TPUs are linear block copolymers consisting of two building blocks: hard segments (HSs) and soft segments (SSs). The HSs are polyurethane blocks, based on diisocyanate and chain extenders, commonly diols, while SS blocks are based on macrodiols, such as polyester, polyether and more recently polycarbonate [2, 3]. The introduction of polycarbonate blocks extended the application to the long term implants in biomedical field, thanks to their higher biostability and biocompatibility [4].

Depending on the thermodynamic incompatibility between HSs and SSs, TPUs are characterized by a phase separation in a soft phase (SP) and a hard phase (HP). In block copolymers characterized by a complete immiscibility, a complete phase separation occurs leading to different morphologies of the bulk, exhibiting a characteristic glass transition temperature (Tg) for each phase [5]. In TPU the phase separation is not complete because of the restriction imposed by the topology of the block copolymers that causes a certain degree of mixing [6]. In addition, the shorter HSs showed to be soluble in the soft phase [7], so the SP contains both HSs and SSs. Consequently, the Tg of the SP will depend on the relative amount of the two different segments and can be predicted with equations such as the Fox equation, in which the Tg of the mixed phase is determined as a combination of the Tg and the weight fractions of the single components of the phase [5, 6].

The hard phase is constitute of polyurethane blocks, ordered on a three dimensional network of hydrogen bonds among the stacked chains, segregating from the soft phase in hard micro-domains [8]. Being those micro-domains linked to the soft phase they act as physical crosslink, determining a typical elastomeric behaviour at room temperature, while retaining thermoplastic processability, subsequently to the heating.

As a consequence of this complex morphology TPUs show multiple thermal transitions in differential scanning calorimetry (DSC) [9]. In addition to the Tg of the SP, other endothermic signals are observed and associated to the short and long range order in the HP [10]. The endotherm at lower temperature (generally referred with T_I) is related to the disordering of the hard micro-domains. [11]. Some authors correlated the value of this temperature to the number of polyurethane

units in the blocks involved in the micro-domain [12, 13]. The short range order, which depends on the thermal history of the polyurethane, can be increased by annealing without affecting any long-range order which may be present [10, 14]. The second endotherm (T_{II}), that is detected at temperature higher than T_I, depends on the copolymer composition and is due to the micro-phase mixing transition, in which the HSs dissolve completely in the SP creating a unique and homogeneous phase [6]. This temperature is independent from the thermal history of the TPU [15].

Some of the transformations observed during thermal treating in DSC can be observed even in FT-IR [16, 17]. Urethane bonds show different carbonyl stretching (1800-1650 cm^{-1}): the absorption peak at lower frequency is referred to strongly hydrogen-bonded carbonyls, while the absorption band at high frequency is assigned to free (not involved in hydrogen bonding) carbonyl groups [18, 19]. Between these two signals are located the vibration of the loosely hydrogen-bonded carbonyls located in the soft phase. On the other hand, hydrogen bond evolution can be even observed in the NH stretching region (3450-3250 cm^{-1}), where a broad band belongs to the stretching of hydrogen bonded N-H groups. The monitoring of the infrared behaviour of these species during thermal treatments allows to evaluate the change in their chemical environment and then in the interaction among the segments.

In literature, several morphological models have been proposed to describe the morphology of TPUs [9, 20, 21]. However, these models are often contradictory, since the morphology of the phases is not universally described, but rather strongly dependent on the amount, size and chemical nature of the different blocks.

Obviously, the phase morphology of a TPU will influence the mechanical behaviour of the material, aim of this work was the study of the effects of thermal treatments on the phase morphology of a PCU developed for medical application, in order to prevent the phase morphology degradation during the medical devices production. Taking into account the thermal stability of polyurethanes [22-24], thermogravimetric measurements have been performed on PCU to evaluate the thermal stability.

2. Experimental

2.1. Materials

The block copolymer commercialized under the trade name of Bionate® is polyurethane, containing a polycarbonate macrodiol as soft segments. The hard segments are based on 4,4'-diphenylmethane-diisocyanate (MDI) and 1,4-butanediol (BD) as chain extender, whereas the soft segments are poly(1,6-hexyl 1,2-ethyl carbonate) diols (PHECD). The chemical structure of this polyurethane is

schematized in Fig. 1. The polycarbonate urethane is produced by DSM PTG (The Polymer Technology Group Inc., Berkley, CA) and commercialized in form of pellet in different hardness grades. The Bionate® studied was a 80A grade.

2.2. Methods.

Thermal degradation was measured in a Hi-Res thermo gravimetric analyzer (TGA Q500 balance, TA Inc.) on 10-15 mg sample contained in alumina pans, with a 10°C/min heating ramp from 50°C up to 800°C under a 100 cm^3/min nitrogen flow (60 cm^3/min sample purge and 40 cm^3/min balance purge). Thermo-oxidation was determined in the same way using a 60 cm^3/min air flow in the sample purge.

A differential scanning calorimeter (DSC Q200, TA Inc.), provided with a cooling system RCS90, was used to collect DSC thermograms. The DSC measurements were performed with closed aluminum pan under nitrogen atmosphere (50 cm^3/min) and with a 20°C/min heating rate, from -75°C up to 220°C cyclically.

To analyze the effect of the temperature on the morphology of the material, annealing experiments were carried out in situ in the DSC apparatus in closed aluminum pan. To evaluate the effect of processing on Bionate, samples were heated at different temperature between 80°C and 220°C and then the morphology was checked.

The infrared measurements were performed with a Perkin Elmer Instrument. FT-IR microscope Spectrum Spotlight 300 was used to collect spectra in reflection-absorption mode on sample held on an aluminium support with a 4 cm^{-1} resolution, 16 scans and area of analysis of 100 x 100 μm. In situ FT-IR were collected during heating in a THMS600 heating/cooling stage (Linkam Scientific Instruments Ltd.) with heating ramp between 30°C to 200°C and 5°C/min heating rate.

ATR-FTIR spectra were recorded on FT-IR spectrometer Spectrum 100 in the attenuated total reflectance (ATR) mode with a diamond crystal, using 16 scans per spectrum and a resolution of 4 cm^{-1}.

3. Results and discussion

3.1 Phases morphology and dependence with temperature.

The DSC curve under a heating ramp ranging from -75°C to 220°C is reported in Fig. 2; Bionate 80A exhibits three thermal phenomena. The first one is a typical step signal due to the glass transition of the soft phase (Tg) and it is centered around -24°C. The curve is then characterized by two endothermic peaks at 110°C (T_I) and 170°C (T_{II}) respectively.

The Tg for polycarbonate homopolymers (Tg_{SS}) composed of similar aliphatic polycarbonate macrodiols have been reported to range from -60 to -40°C. The Tg value detected for the soft phase is higher than the Tg_{SS}, indicating that the soft phase is composed of SSs mixed with a certain amount of polyurethane HSs. The relative amount of each blocks in the soft phase has been calculated with the Fox equation, modified for polyurethanes [6]:

$$(W_{SS}+kW_{HS})/Tg = W_{SS}/Tg_{SS}+ kW_{HS}/Tg_{HS}$$

Considering a value of 110°C for the Tg of polyurethane homopolymer [25] and the Tg_{SS} ranging from -60 to -40°C, with k=1.18, the soft phase will contains from 14 to 28% wt of polyurethanes HS.

Even if it is not due to the melting of a conventional crystalline phase composed of polymer chains folded to form discrete crystallite structures the endoderm at T_I is, however, a sign of the presence of highly ordered structures. On the other hand T_I is strongly dependent from the thermal history and strictly related to the temperature at which a sample has been stored or equilibrated [11, 12].

The T_{II} endotherm is associated to the dissolution of the segregated HSs with the SSs matrix to create a homogeneous phase [9], this is the temperature at which the polyurethane blocks became thermodynamically compatible with the soft segments block and it is not affected by the thermal history of the polymer.

The study of the dependence from thermal history of bulk morphology has been divided among heating above T_{II}, the temperature necessary to process PCU, and below this temperature, namely in the range of storage and post processing.

3.1.1 Effect of heating above the processing temperature.

Samples have been heated up to 220°C, cooled to -75°C and then reheated to 220°C at 20°C/min (Fig. 3, A). In the second heating ramp the Tg is shifted from -24°C to 0°C, indicating an increase of polyurethane HSs in the SP. Appling the Fox equation the amount of HSs is about 15% higher in the second heating than the amount calculated for the first heating. The value obtained in this case can be considered the overall amount of PU in the Bionate 80A. Indeed, during the cooling there is no evidence of any exothermic signal, suggesting a reverse phenomenon of the phase mixing, so the morphology of the bulk can be considered composed of a single amorphous phases, containing all the HSs and SSs. However, this phase is due to the fast cooling and is unstable: the exothermic peak above 50°C in the second heating ramp denotes a de-mixing process after which a more thermodynamically stable SP, containing less HSs, is formed. Performing a slower cooling ramp

(5°C/min, Fig 3B), an exothermic peak due to the heat released by the de-mixing is detected at 70°C. Both these exothermic phenomena (labeled T_{II}') are related to the same process. After the slower cooling the Tg is below the Tg of the completely mixed phase but still above that of the untreated Bionate, indicating an higher amount of HSs in comparison with the pristine materials. Considering T_I signal, it is interesting to note that in the second ramp it is not detected, whatever is the cooling ramp, meaning that even if a certain amount of HS are segregated from the soft matrix, they are not able in the circumstances of the experiment to organize them self to form ordered structures.

The amorphous monophase obtained with the quenching is unstable even at temperatures lower than that needed for the de-mixing under heating. In Fig. 4 are reported the DSC thermograms of samples quenched to ambient temperature after being heated above the T_{II}. After 5 minutes of aging the sample shows the presence of a single amorphous phase, but after 30 minutes a shifting to lower temperature of the Tg indicates that the de-mixing process occurred at ambient temperature. The soft phase has a lower amount of HSs, which is segregated in hard micro-phases. This is not surprising since being over the glass temperature the chains have the necessary mobility to segregate. The time needed to complete the segregation will depend on the temperature that macroscopically regulate the viscosity of the phase in according with Williams-Landel-Ferry equation [26]. The exothermic peak of de-mixing disappears after one day. For longer aging time the Tg remain almost the same indicating that after one day the relative amount of HS and SS in the matrix reached an equilibrium. After one day the T_I peak around 60°C appears, demonstrating the formation of ordered structures in the hard micro-phases, due to the reorganization of the polyurethane segments present in these segregation areas. Increasing the aging time this peak became more evident and shifts to higher temperature indicating an increase in the amount of micro-domains and an increase of their dimensions respectively. The higher temperature reached for T_I peak is 80°C after two months. Longer aging time have no influence on DSC curve of PCU.

The FT-IR study of the hydrogen bond between the polymer chains confirms this interpretation. In Fig. 5 are reported the FT-IR spectra in the C=O and N-H stretching regions registered on a PCU film during heating from 30°C to 200°C at 5°C/min. In the carbonyl region there should be a total of five different carbonyl FTIR vibrations: two signals for the not involved in hydrogen bonding urethane and carbonate carbonyls, two signals for those involved in hydrogen bonding and contained in the soft phase, one signal for ordered hydrogen bonding urethane carbonyls in the hard phase [18]. Being the absorption frequency very close, the overlapping of these absorption peaks results in a broad multiple peak as can be seen in Fig. 5, on the right. The broad signal I_{CO} centred at 1737 cm^{-1} has been assigned to free (not involved in hydrogen bonding) carbonyls of the carbonate

and urethane groups; a multiple shoulder (II_{CO}) at 1722 cm^{-1} to hydrogen-bonded carbonyls of both carbonate and urethane groups in the amorphous phase, while the signal III_{CO} at 1700 cm^{-1} has been attributed to strongly hydrogen-bonded carbonyls of the urethane group in the ordered hard domains [18]. In the left side of Fig. 5, the stretching of the NH signal is also affected by the presence of the intermolecular interaction: the NH stretching (III_{NH}) at 3336 cm^{-1} is assigned to this group involved in hydrogen bonds. At 3392 cm^{-1} there is a low shoulder (II_{NH}), related to the NH group involved in hydrogen bond interaction in the amorphous phase, mainly with the carbonate carbonyls. The absence of signals at higher frequency suggests that almost all the NH groups are involved in hydrogen bonding interactions.

During the heating, all the signals are affected by the temperature that induces changes in the chemical environment. Nevertheless, the main changes are on the groups directly involved in the hydrogen bonding interaction. The alterations of the signals in the C=O and N-H stretching regions give information on the effect of the thermal treatment on the morphology of the PCU. In the carbonyl region, the signal III_{CO} at 1700 cm^{-1} increases with the heating temperature to 100°C, sign of an increase of the urethane carbonyls involved in hydrogen bond in the hard micro-domain, thanks to the reorganization of the HSs. Over this temperature the signal decreases with the increase of the temperature and at 150°C the III_{CO} signal disappears completely. Over 100°C, the breakdown of the hydrogen bonds induces the disruption of the short range order and the loss of organization in the micro-domains. Comparing the infrared evidences with the first cycle of the DSC curve reported in Fig. 3B, 100°C is the starting temperature of the disruption of the short range order (T_I peak), temperature at which the interaction in the micro-domain are destroyed and the shorter HSs begins to dissolve in the matrix. The decreasing of the peak III_{CO} is accompanied with the increase of the signals I_{CO} and II_{CO}. The signal I_{CO} at 1737 cm^{-1} is also shifted to a lower frequency (1742 cm^{-1}). For temperature over 150°C, the spectra do not change anymore with the heating.

The biphasic morphology is lost during the mixing that takes place starting from 150°C. The infrared spectra confirm DSC data: the amount of the free species increases and the signal III_{CO}, related to the short range order disappear above this temperature. The same behaviour observed for the carbonyl is detected also for the NH stretching. The signal III_{NH} related to the species involved in the strongly hydrogen-bond in the hard domain decreases and shifts from 3336 cm^{-1} to 3364 cm^{-1}; the signal II_{NH} at 3400 cm^{-1}, very low before the heating, increases; a new signal related to the NH group not involved in hydrogen bond (I_{NH}) appears at 3440 cm^{-1}.

In Fig. 6, the FT-IR spectra under cooling from 200°C to 30°C in the C=O (right) and N-H (left) stretching regions are reported. Cooling causes reverse phenomena but, as seen in DSC, the recovery is not complete. The I_{CO} and I_{NH} signals decrease, due to decrease of species not involved

in hydrogen bonding. The III_{NH} at 3364 cm^{-1} shift to 3340 cm^{-1}. In the carbonyl region only at low temperature (below 60°C) it is possible to detect the III_{CO} signal, referable to the ordered hydrogen bond. This is another confirmation of the kinetic dependence of T'_{II}: during the cooling the HSs segregate in the hard phases. After the cooling the II_{CO} and II_{NH} absorptions correlated to the interaction in the soft phase are still higher than in the starting material: the organization of the morphology is different in comparison with the one observed before the heating. Even if the de-mixing happens the segregation of the hard segments from the matrix does not induce immediately the formation of the ordered structures seen prior to the thermal treatment. Few HSs are involved in the ordered hydrogen bond of the micro-domain confirming the absence in DSC of the T_I signal in the second heating ramp.

Providing longer time to PCU to relax after heating the infrared signal continues to evolve. In Fig. 7 ATR spectra collected over time are reported. The infrared spectra were performed on sample heated over T_{II} and then quenched at ambient temperature. The signals II_{CO} and II_{NH} decrease, because of the decrease of HSs to give loosely hydrogen-bonded carbonyls in the amorphous phase. The III_{CO} and III_{NH} signals increase, sign that ordered hydrogen bond are forming during the aging. The III_{NH} signal shifts form 3342 cm^{-1} to 3335 cm^{-1}, the starting value. The evolution of PCU continue after the cooling at room temperature: being above the glass transition the mobility of chains segments allows HSs to segregate from the soft phase and to form the hard phases and from there ordered micro domains. The HSs tend to assume conformations that facilitate the packing of the molecules, and that allow the hydrogen bonding among them. The DSC curve collected on the samples after the last spectrum reported in Fig. 7 exhibits DSC very similar to the last DSC curve detected after two months of aging.

3.1.2 Effect of annealing treatment at temperature below the processing temperature.

In order to investigate the dependence between temperature and the dimensions of the ordered hard micro-domains, different specimens have been heated at different temperature from 100°C to 200°C. After these annealing the samples were cooled to -75°C and the subsequent DSC heating ramps are reported in Fig. 8. The higher is the annealing temperature, the higher is T_I evidencing an increase in the dimension of the micro-domains. This behaviour has been already observed for TPU based on polyether SS [11, 21]. If the annealing occurs at 170°C the micro-domains are so extended that a temperature higher than the demixing temperature is needed to be melted. Heating at temperature higher than 170°C, the sample is above the mixing temperature and no ordered structures are formed, as can be showed by thermograms obtained after annealing at 180°C and 200°C respectively. The Tg seems to be slightly influenced by the annealing showing a non linear

increase with the increase of the annealing temperature. During annealing, the polyurethane segments in the hard micro-domain acquire the necessary mobility to reorganize in bigger domain while the shorter hard segment is allowed to dissolve in the soft phase, increasing the Tg.

The T_{II} temperature is located at the same temperature in all cases, confirming the independence of mixing from the thermal history.

The ATR-FTIR spectra of annealed and then quenched samples support this hypothesis and confirm the results obtained in DSC. In Fig. 9, the carbonyl stretching region of the samples annealed at 80°C, 100°C and 120°C is reported. The increase of III_{CO} peak, detected for the sample heated up to 100°C, and the same T_I in the DSC of those samples supports the hypothesis of an increase in the amount of three dimensional networks, but not their dimension. In the samples annealed at 120°C, because of the disruption of the three dimensional network of hydrogen bonding, confirmed by the decrease of III_{CO} peak, the HSs in the micro-domain can reorganize and form bigger ordered structures, that are destroyed at higher temperature.

T_I is affected also by the annealing time: the longer is the time spent at certain temperature, the higher is the temperature for the micro-domains melting. In Fig. 10 is reported the comparison of the T_I values obtained for treatments performed at the same temperatures but annealed with and without 30 minutes of isotherm. Later on the isotherm, the samples exhibit higher T_I, which means bigger dimension of micro-domains.

3.2 Thermal stability

The thermo gravimetric analyses (TGA) performed in inert and oxidative atmosphere are compared in Fig. 11. Under N_2 the polymer shows a main step of weight loss between 230°C and 380°C. At the end of this step a low amount of residue of 5% wt. is left. This residue is completely volatilized between 380°C and 470°C. The effect of heat on the chain is believed to take place on the urethanes bond. It is well know that the urethane bond is subjected to rupture under heating starting to relatively low temperature (i.e. 150°C) but this reaction is counterbalanced by a recombination. This phenomenon is known as trans-urethanization. At higher temperature the equilibrium shifted towards the dissociation of the urethane bond and volatile low molecular mass fragments are the main process products.

Under air flow the TPU shows a fairly uncommon behaviour. Polymers that thermally degrade with free radical chain reaction show in presence of oxygen a destabilization effect due to the high reactivity of oxygen with macroradicals that leads to the formation of thermally unstable species. On the other hands polymers that thermally degrade with reaction that do not involve formation of macroradicals are not affected by the presence of oxygen, showing TGA curves with no significant

difference between Air and Nitrogen in term of thermal stability. Oddly, Bionate 80A is stabilized by the presence of oxygen that seems to interact with the volatilization mechanism shifting to higher temperature the mass fragmentation. However the amount of residue produced is higher in air. This is a typical behaviour for many polymers: in this range of temperature the presence of oxygen promotes the formation of char through oxidative dehydrogenation process [27]. Persisting with the heating ramp, under air, this residue will be completely volatilized through combustion reaction at temperature above 500°C. The onset temperatures of the degradation steps and the amount of residues at different temperatures are reported in Table 1.

Comparing the temperature obtained from TGA and DSC results, it is possible to notice that the temperature needed to create a homogeneous melt is close to the temperature at which thermal degradation starts. To process this material it is necessary take into account both these conditions. In addition, the temperature at which the weight loss becomes evident, is not directly connected with the degradation temperature, side reactions can take place also before, without the formation of any volatile products. The processing must be controlled, since it can be a very important step to maintain the chemical features of the copolymer.

4. Conclusion

The physical properties of Bionate are strongly affected by the thermal history. At room temperature Bionate 80A is composed of urethanic hard micro-domains dispersed in a soft phase, containing both urethane and carbonate blocks. The heating above the processing temperature lead to the complete mixing, inducing the formation of a unique phase in which HSs and SSs are dispersed. This monophasic system can be preserved with a quenching but, being unstable, a demixing process takes place at temperature above the glass transition temperature. The segregation of the HSs from the soft phase leads to the formation of a hard phase organized in hard micro-domains. DSC and FT-IR results evidenced that the dimensions and the amount of these hard micro-domain strongly depends on thermal history during processing.

This lead to hypothesize that mechanical properties of Bionate 80A can be modulated controlling the annealing conditions during process. However, aging experiments demonstrated that above the glass transition the biphasic morphology undergoes modification until an equilibrium state is not reached. This is of paramount importance considering biomedical applications, suggesting that mechanical properties of PCU should be evaluated in condition corresponding to those of human body.

TGA experiments demonstrated that the degradation temperature is very close to the temperature at which PCU are processed. In these conditions, where mechanical stress due to machinery such as extruders can be very strong, the risks of degradation should be carefully taken in account.

References

[1] Hepburn C. Polyurethane Elastomers. Second ed. Great Yarmouth: Elsevier Applied Science; 1992.
[2] Petrovic ZS, Ferguson J. Polyurethane Elastomers. Progress in Polymer Science. 1991;16:695-836.
[3] Krol P. Synthesis methods, chemical structures and phase structures of linear polyurethanes. Properties and applications of linear polyurethanes in polyurethane elastomers, copolymers and ionomers. Progress in Materials Science. 2007;52:915-1015.
[4] Stokes K, Mcvenes R, Anderson JM. Polyurethane Elastomer Biostability. Journal of Biomaterials Applications. 1995;9:321-54.
[5] Wood LA. Glass Transition Temperature of Copolymers. Journal of Polymer Science. 1958;28:319-30.
[6] Leung LM, Koberstein JT. Dsc Annealing Study of Microphase Separation and Multiple Endothermic Behavior in Polyether-Based Polyurethane Block Copolymers. Macromolecules. 1986;19:706-13.
[7] Runt J, Garrett JT, Lin JS. Microphase separation of segmented poly(urethane urea) block copolymers. Macromolecules. 2000;33:6353-9.
[8] Blackwell J, Nagarajan MR, Hoitink TB. Structure of polyurethane elastomers. X-ray diffraction and conformational analysis of MDI-propandiol and MDI-ethylene glycol hard segments. Polymer. 1981;22:1534-9.
[9] Saiani A, Rochas C, Eeckhaut G, Daunch WA, Leenslag JW, Higgins JS. Origin of multiple melting endotherms in a high hard block content polyurethane. 2. Structural investigation. Macromolecules. 2004;37:1411-21.
[10] Seymour RW, Cooper SL. Thermal Analysis of Polyurethane Block Polymers. Macromolecules. 1973;6:48-53.
[11] Martin DJ, Meijs GF, Gunatillake PA, McCarthy SJ, Renwick GM. The effect of average soft segment length on morphology and properties of a series of polyurethane elastomers .2. SAXS-DSC annealing study. Journal of Applied Polymer Science. 1997;64:803-17.
[12] Martin DJ, Meijs GF, Renwick GM, McCarthy SJ, Gunatillake PA. The effect of average soft segment length on morphology and properties of a series of polyurethane elastomers .1. Characterization of the series. Journal of Applied Polymer Science. 1996;62:1377-86.
[13] Harrell LL. Segmented Polyurethans. Properties as a Funcation of Segment Size and Distribution. Macromolecules. 1969;2:607-12.
[14] Miller JA, Lin SB, Hwang KKS, Wu KS, Gibson PE, Cooper SL. Properties of polyether-polyurethane block copolymers: effects of hard segment length distribution. Macromolecules. 1985;18:32-44.
[15] Saiani A, Daunch WA, Verbeke H, Leenslag JW, Higgins JS. Origin of multiple melting endotherms in a high hard block content polyurethane. 1. Thermodynamic investigation. Macromolecules. 2001;34:9059-68.
[16] Koberstein JT, Gancarz I, Clarke TC. The Effects of Morphological Transitions on Hydrogen-Bonding in Polyurethanes - Preliminary-Results of Simultaneous Dsc-Ftir Experiments. Journal of Polymer Science Part B-Polymer Physics. 1986;24:2487-98.
[17] Spirkova M, Pavlicevic J, Strachota A, Poreba R, Bera O, Kapralkova L, et al. Novel polycarbonate-based polyurethane elastomers: Composition-property relationship. European Polymer Journal. 2011;47:959-72.

[18] Runt J, Pongkitwitoon S, Hernandez R, Weksler J, Padsalgikar A, Choi T. Temperature dependent microphase mixing of model polyurethanes with different intersegment compatibilities. Polymer. 2009;50:6305-11.
[19] Seymour RW, Estes GM, Cooper SL. Infrared Studies of Segmented Polyurethan Elastomers. I. Hydrogen Bonding. Macromolecules. 1970;3:579-83.
[20] Lee HS, Wang YK, Hsu SL. Spectroscopic Analysis of Phase-Separation Behavior of Model Polyurethanes. Macromolecules. 1987;20:2089-95.
[21] Koberstein JT, Russell TP. Simultaneous Saxs-Dsc Study of Multiple Endothermic Behavior in Polyether-Based Polyurethane Block Copolymers. Macromolecules. 1986;19:714-20.
[22] Hentschel T, Munstedt H. Kinetics of the molar mass decrease in a polyurethane melt: a rheological study. Polymer. 2001;42:3195-203.
[23] Grassie N, Zulfiqar M. Thermal degradation of the polyurethane from 1,4-butanediol and methylene bis(4-phenyl isocyanate). Journal of Polymer Science: Polymer Chemistry Edition. 1978;16:1563-74.
[24] Yang WP, Macosko CW, Wellinghoff ST. Thermal-Degradation of Urethanes Based on 4,4'-Diphenylmethane Diisocyanate and 1,4-Butanediol (Mdi/Bdo). Polymer. 1986;27:1235-40.
[25] Chen TK, Chui JY, Shieh TS. Glass transition behaviors of a polyurethane hard segment based on 4,4'-diisocyanatodiphenylmethane and 1,4-butanediol and the calculation of microdomain composition. Macromolecules. 1997;30:5068-74.
[26] Williams ML, Landel RF, Ferry JD. The Temperature Dependence of Relaxation Mechanisms in Amorphous Polymers and Other Glass-forming Liquids. Journal of the American Chemical Society. 1955;77:3701-7.
[27] Benson SW, Nangia PS. Some unresolved problems in oxidation and combustion. Accounts of Chemical Research. 1979;12:223-8.

Figure Captions

Fig. 1 Chemical structure of Bionate 80A.

Fig. 2 DSC curve of Bionate 80A, first heating from -75°C to 220°C at 20°C/min

Fig. 3 Two consecutive cycle of DSC A) at 20°C/min; B) at 5°C/min

Fig. 4 DSC curves of samples heated over processing temperature and then quenched at ambient temperature collected at different storage time.

Fig. 5 FTIR spectra collected during heating from 30°C to 200°C at 5°C/min in the NH (left) and CO (right) stretching regions.

Fig. 6 FTIR spectra collected during cooling from 200°C to 30°C at 5°C/min in the NH (left) and CO (right) stretching regions.

Fig. 7 ATR-FTIR spectra collected during aging after heating over processing temperature in the CO stretching region.

Fig. 8 DSC curves of samples annealed at different temperature and then cooled at -75°C

Fig. 9 ATR-FTIR spectra in the CO stretching region of samples annealed at different temperature and then cooled at -75°C.

Fig. 10 Comparison of the T_I values for samples annealed at different temperature with or without 30 minutes of isotherm.

Fig. 11 Thermogram of Bionate in air and nitrogen atmosphere

Tables

Table 1 Degradation temperature of inflection point and residue in air and nitrogen for Bionate 80A.

	Temperature (°C)			Residues (%)		
	1st step	2nd step	3rd step	At 400°C	At 500°C	At 700°C
air	359	420	560	15%	13%	0%
nitrogen	352	433	559	3.2%		1.1%

Figure1

Click here to download high resolution image

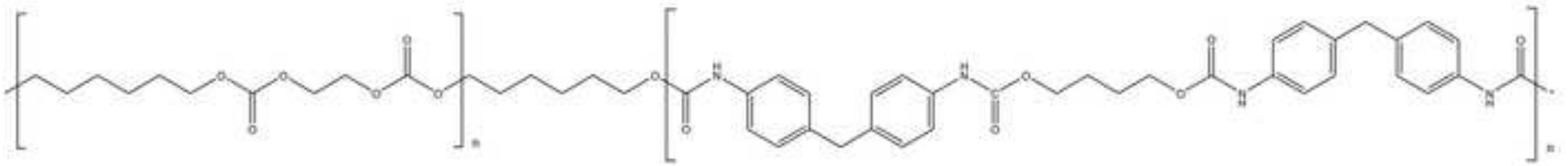

Figure2

Click here to download high resolution image

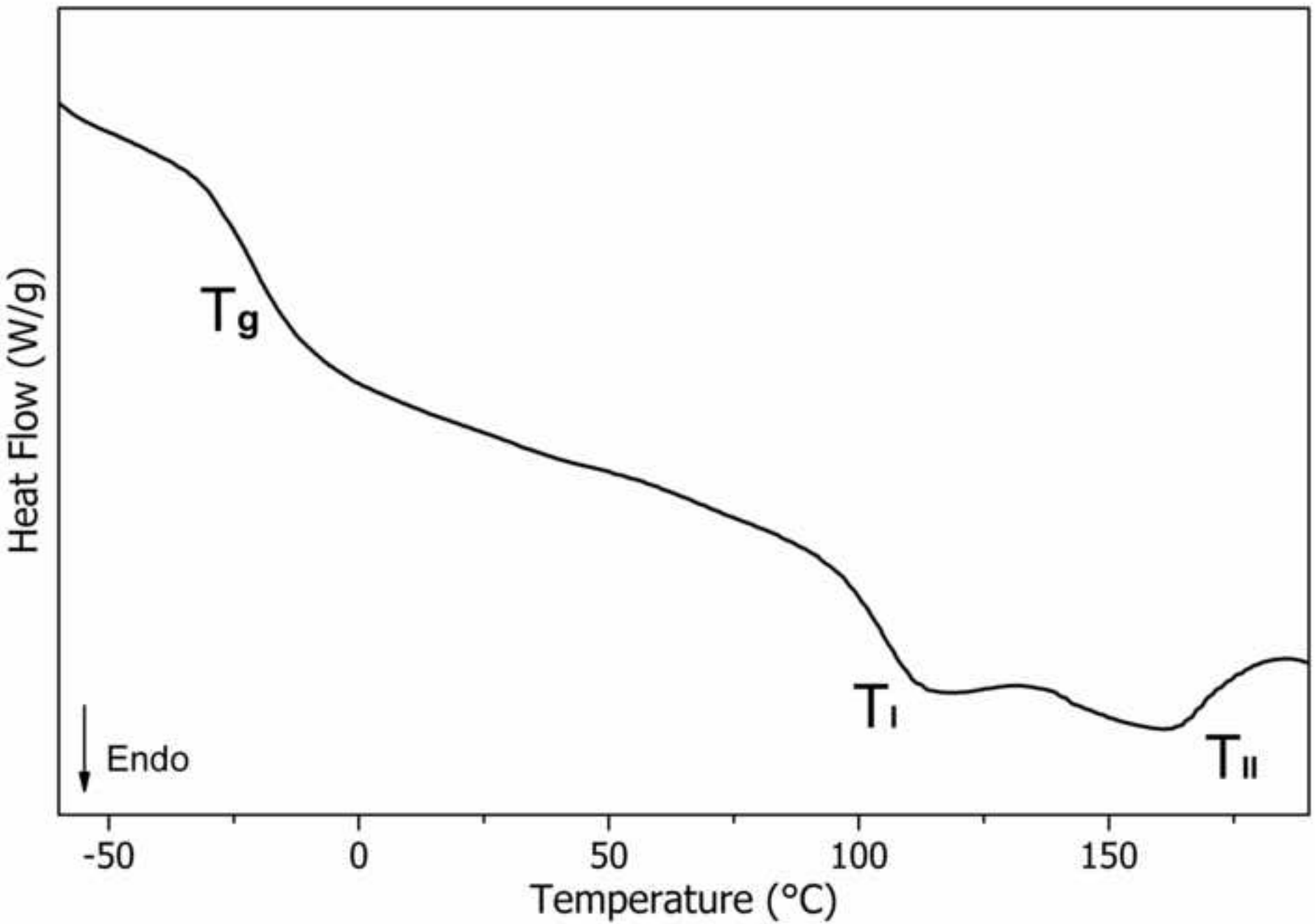

Figure3

Click here to download high resolution image

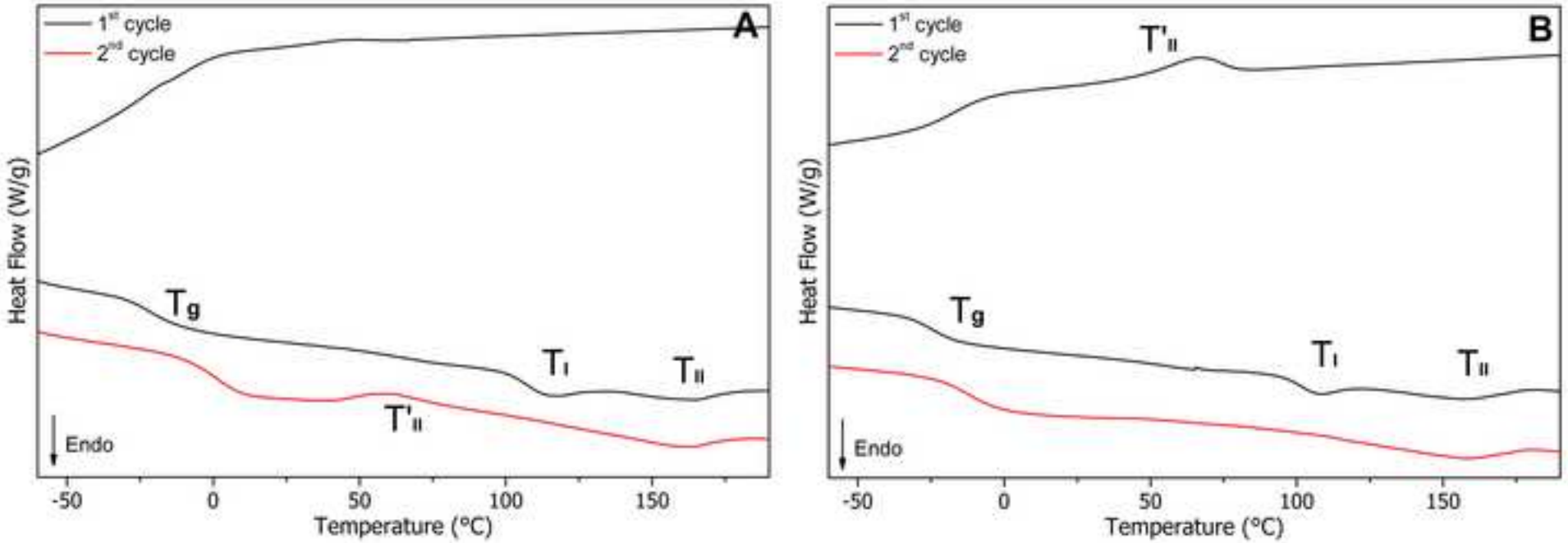

Figure4

Click here to download high resolution image

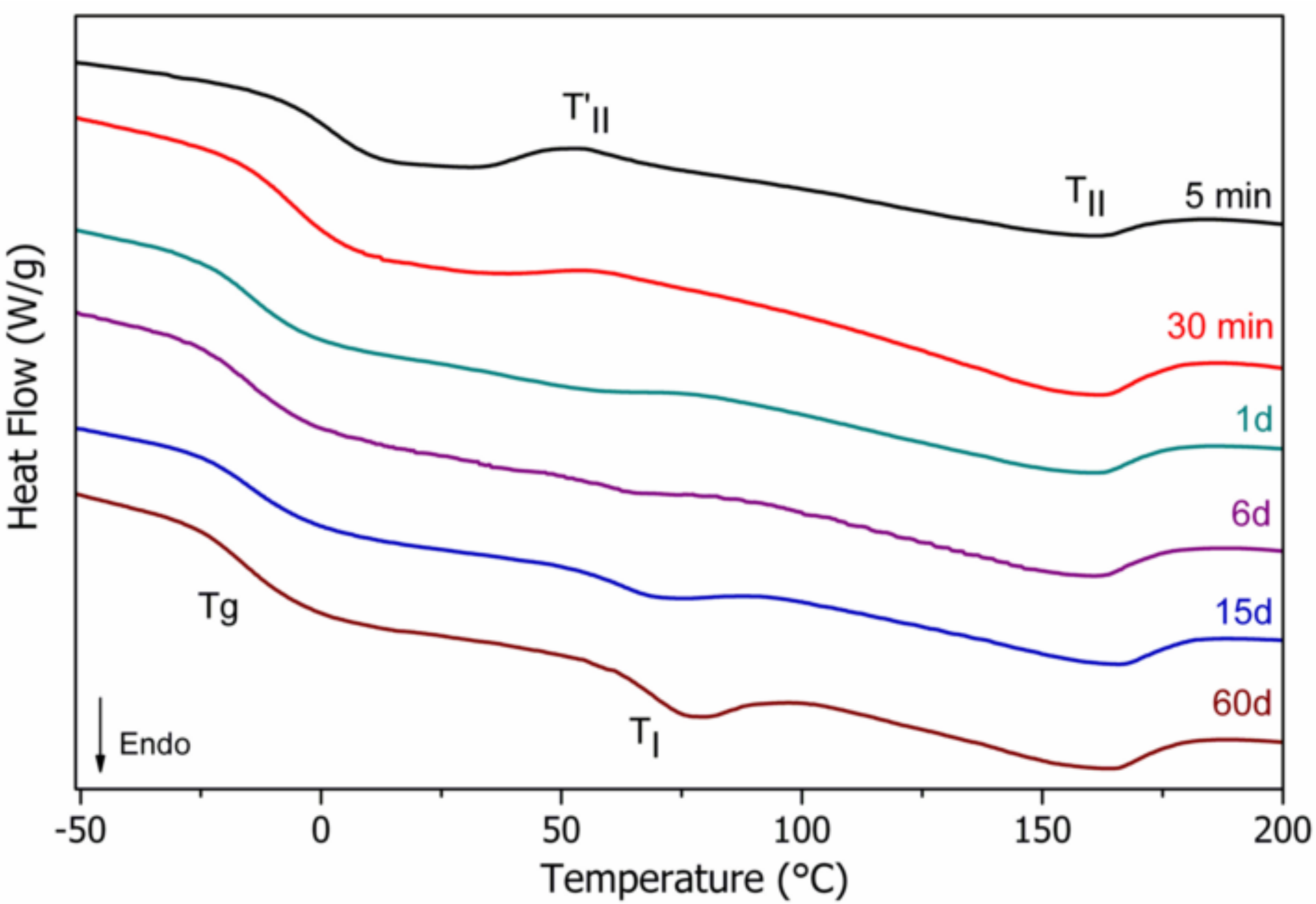

Figure5

Click here to download high resolution image

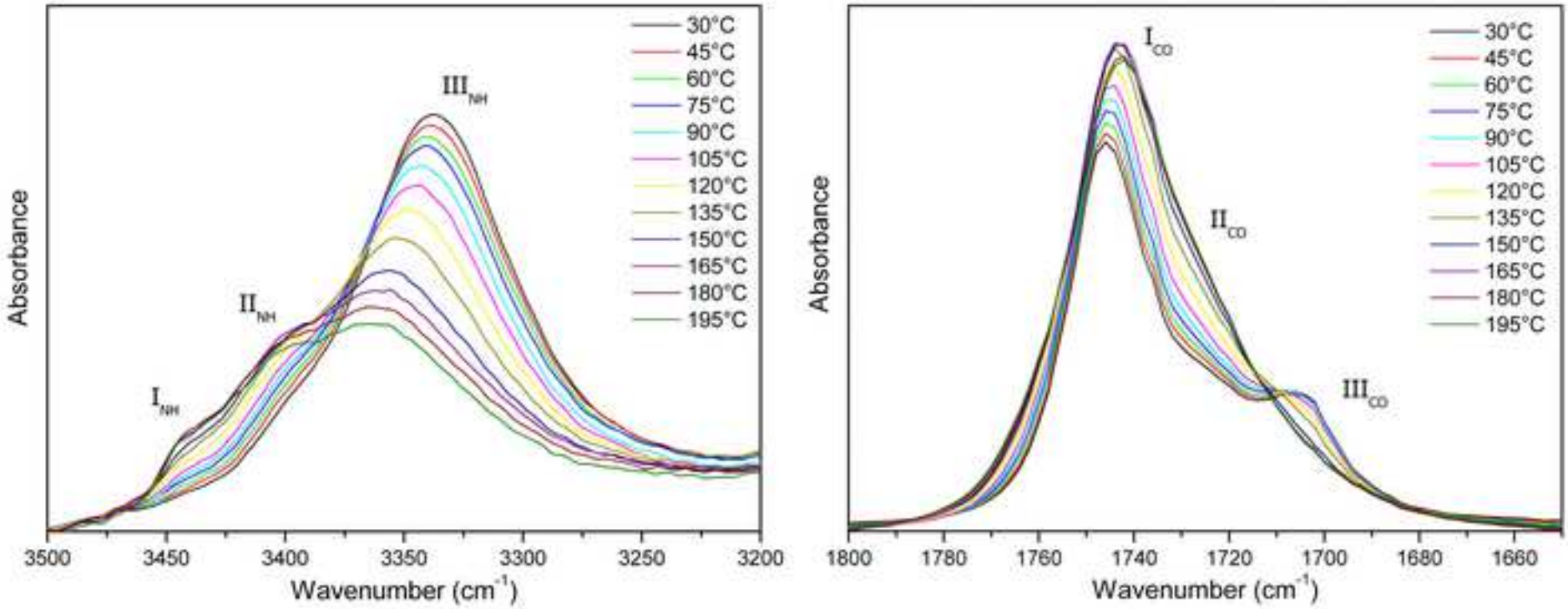

Figure6

Click here to download high resolution image

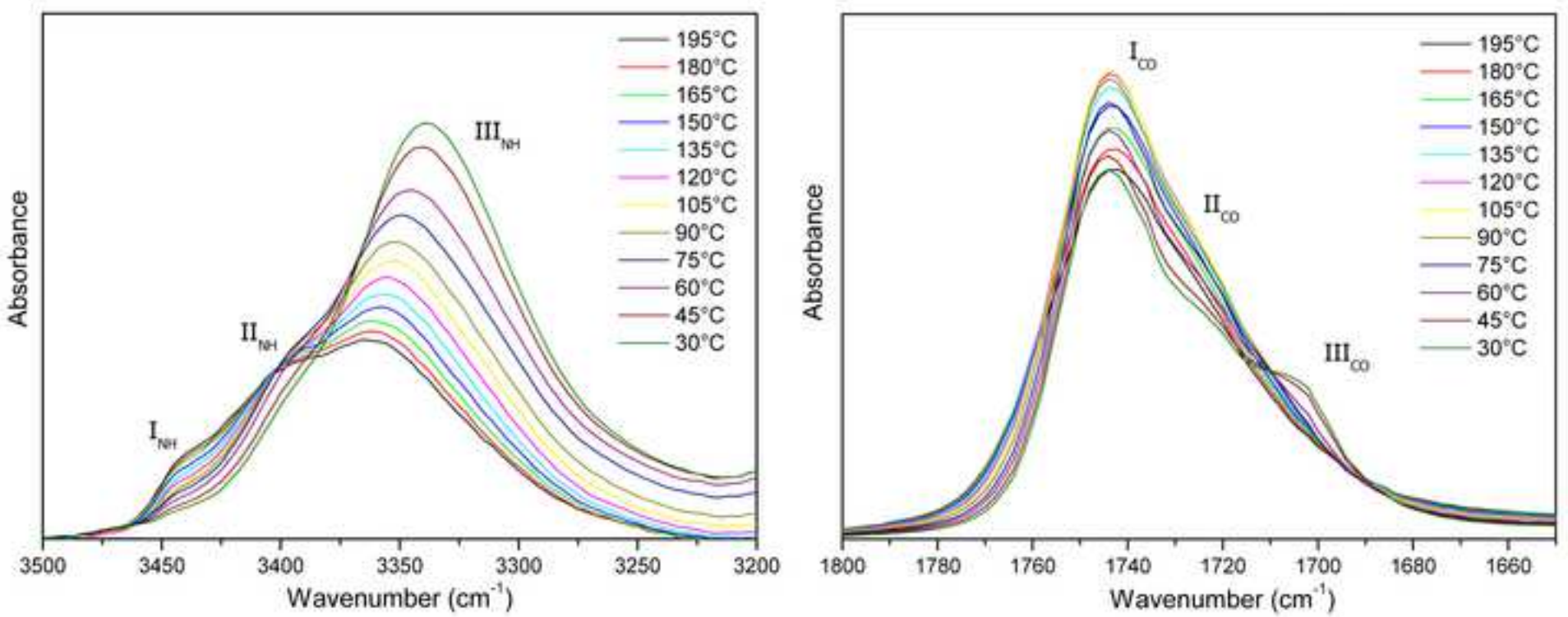

Figure7

Click here to download high resolution image

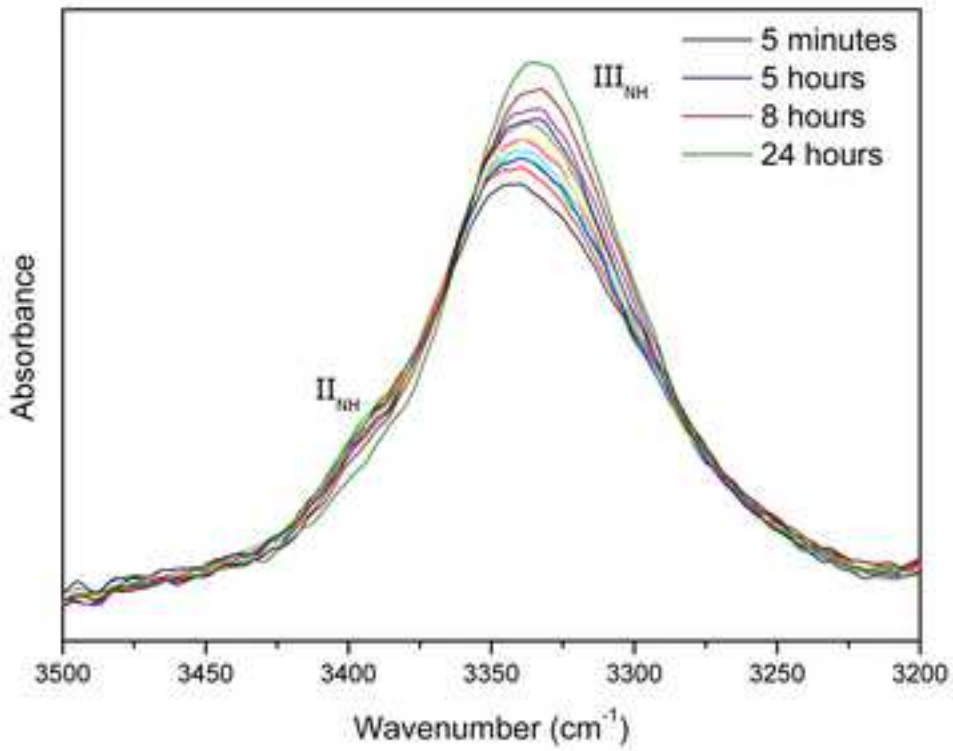

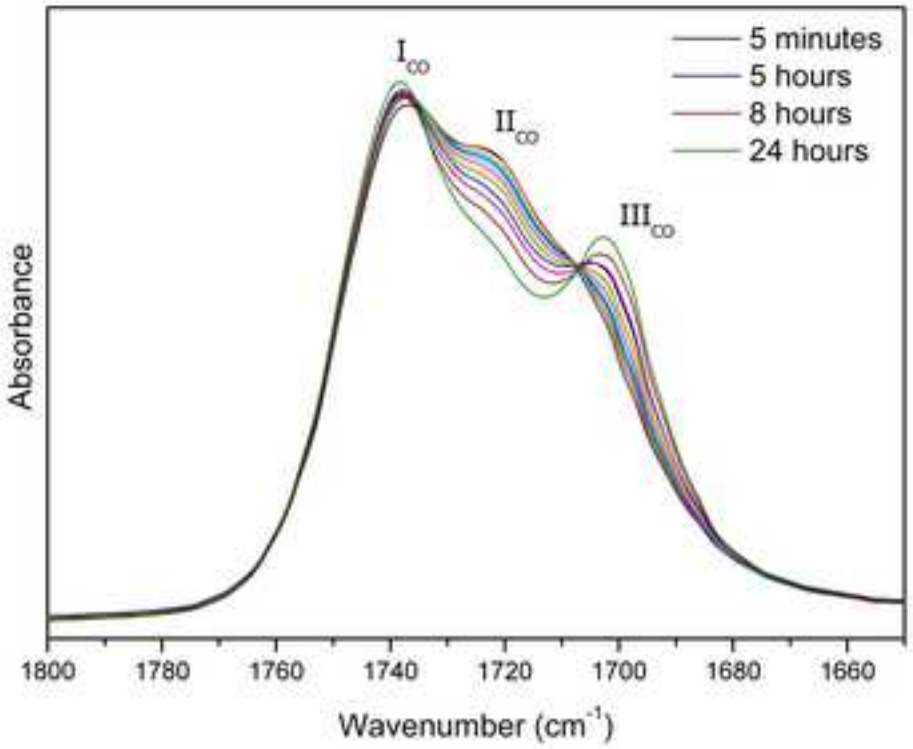

Figure8

Click here to download high resolution image

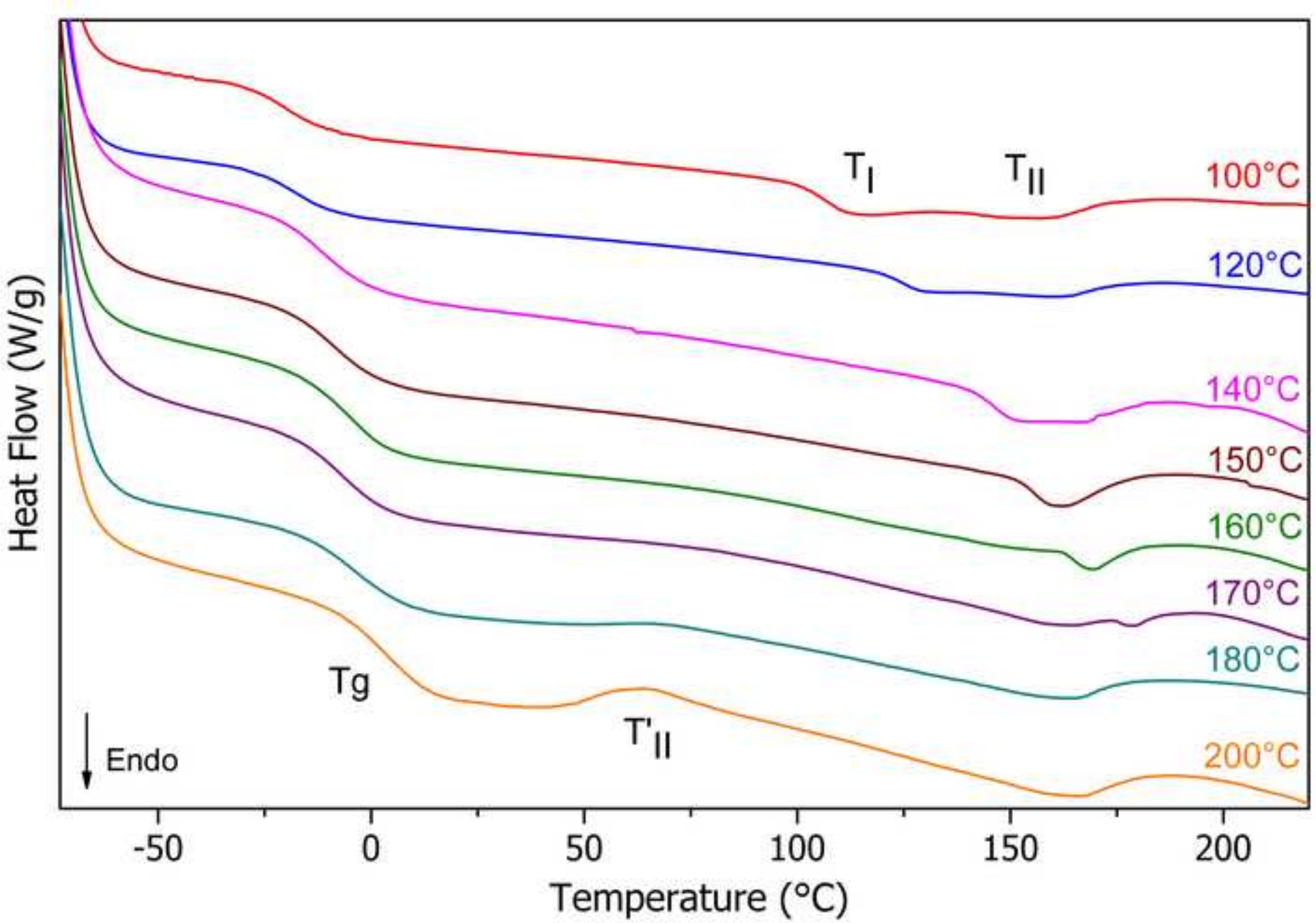

Figure9

Click here to download high resolution image

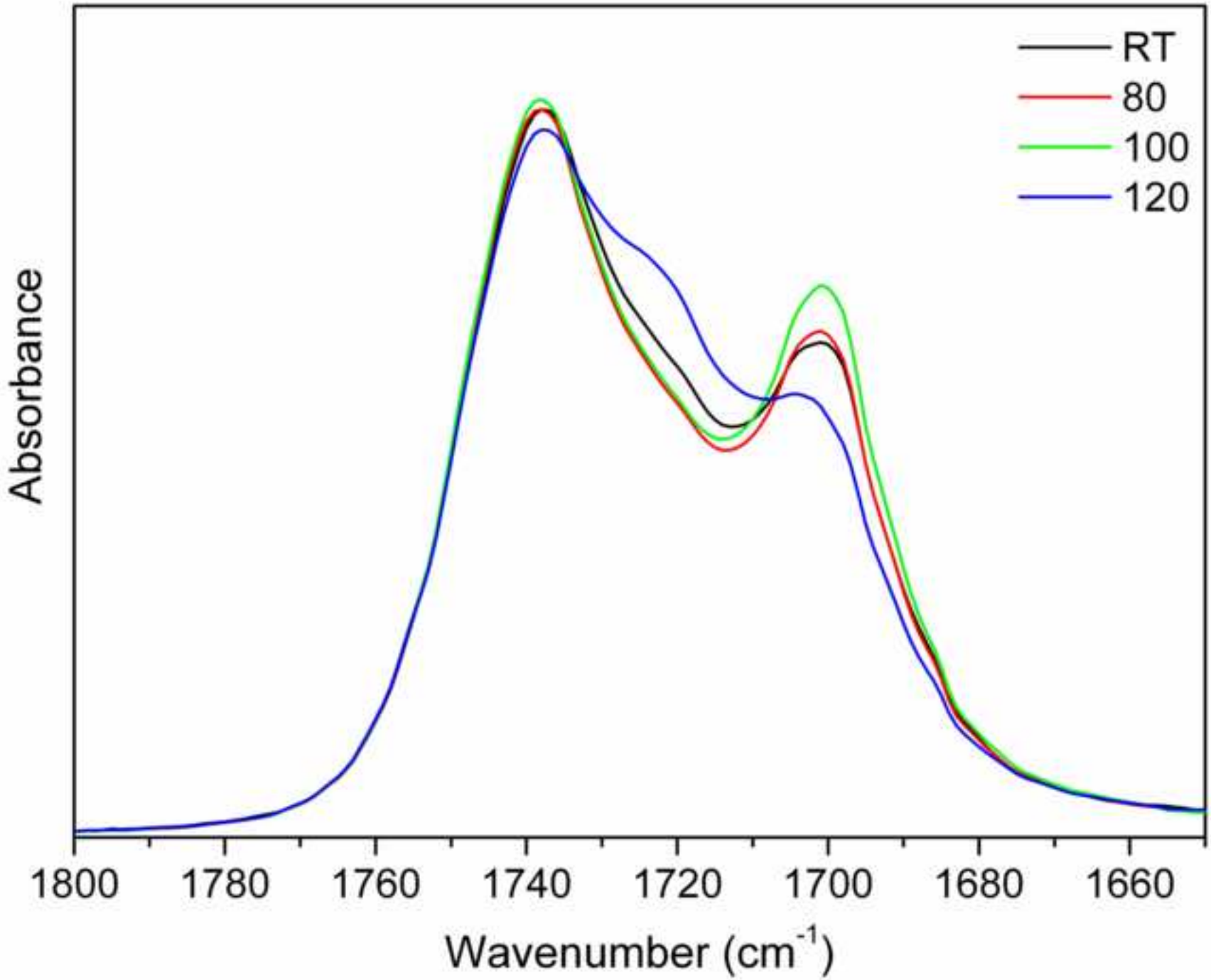

Figure10

Click here to download high resolution image

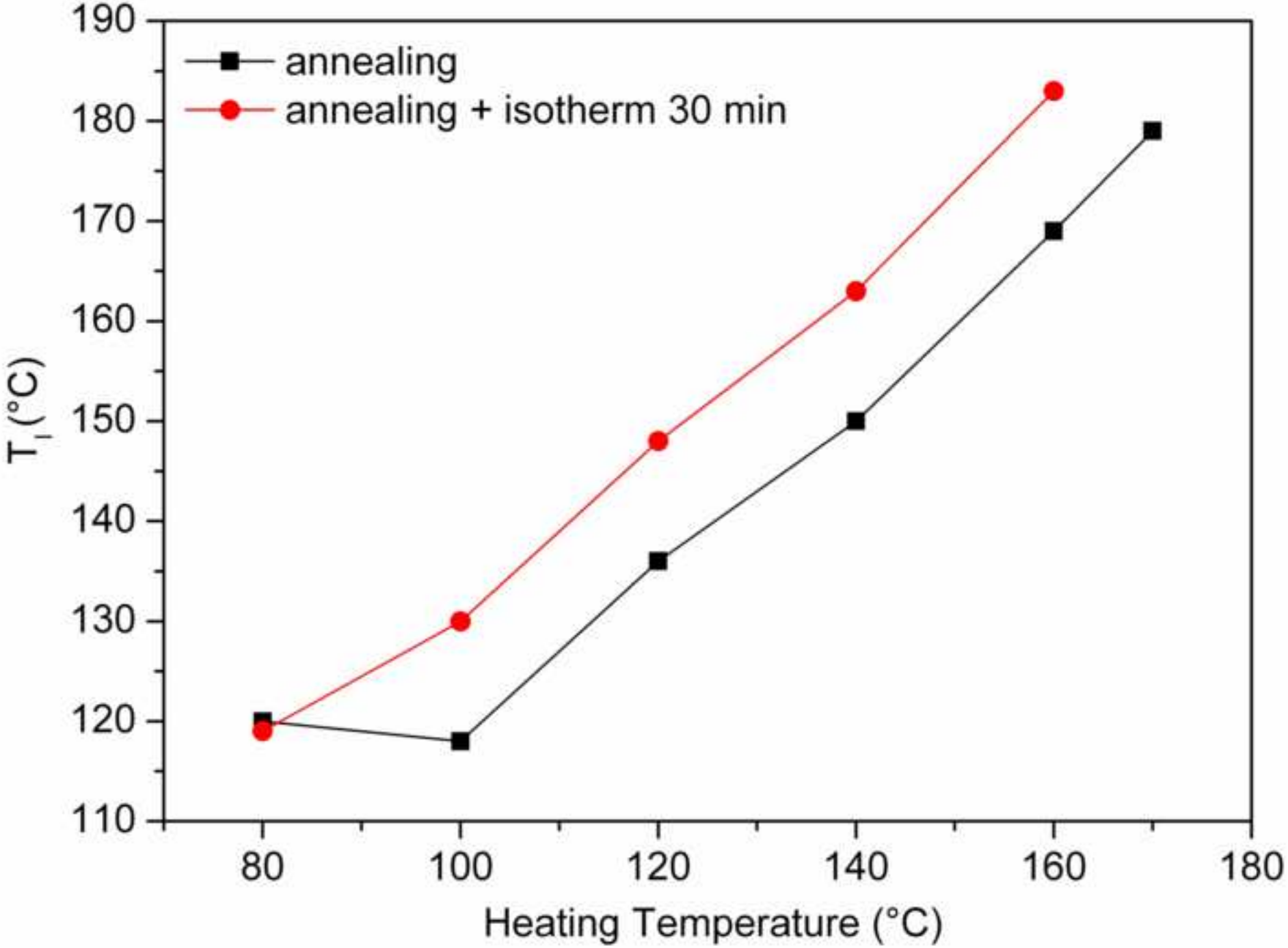

Figure11

Click here to download high resolution image